BIOCHEMISTRY
including biophysical chemistry & molecular biology
Rapid Report

Biochemistry **2010,** *49,* 1361–1363 1361
DOI: 10.1021/bi9014693

Kinetics of the Transfer of Ubiquitin from UbcH7 to E6AP

Carrie Purbeck,[‡] Ziad M. Eletr,[‡] and Brian Kuhlman*

Department of Biochemistry and Biophysics, University of North Carolina, Chapel Hill, North Carolina 27599-7260
[‡]*These authors contributed equally to this work.*

Received August 21, 2009; Revised Manuscript Received December 21, 2009

ABSTRACT: Prior to substrate ubiquitination by HECT-E3 ligases, ubiquitin must first be activated by E1 and then transferred via a series of transthiolation reactions from E1 to E2 and from E2 to E3. We have measured the rate constants and binding affinities underlying the transfer of ubiquitin from E2 UbcH7 to the HECT domain of E3 E6AP. We show that charged UbcH7 and free UbcH7 bind E6AP with similar affinities and that at 37 °C the second-order rate constant for the reaction (k_{cat}/K_m) equals $\sim 2.3 \times 10^5$ M^{-1} s^{-1}. The measured parameters place limits on substrate−E6AP binding lifetimes required for processive polyubiquitination.

Ub is conjugated to lysine side chains of protein substrates through sequential enzymatic reactions performed by an activating enzyme (E1), conjugating enzymes (E2), and ligases (E3) (*1*, *2*). E1 uses ATP to adenylate the C-terminal carboxylate of Ub (G76); once activated, Ub is capable of forming thioester-bonded intermediates between G76 and the catalytic cysteine residues of E1, E2, and HECT-E3 enzymes. Two transthiolation reactions, between E1 and E2 and between E2 and HECT-E3, produce a Ub∼HECT-E3 intermediate (∼ denotes a thioester bond) primed to tether Ub onto a substrate. In the simplest scenario, a lysine residue of the E3-bound substrate attacks the Ub∼HECT-E3 thioester, resulting in transfer of Ub and an isopeptide bond between the N^{ζ} lysine atom and G76. Monoubiquitination, or the attachment of a single Ub to a substrate, has been demonstrated by HECT-E3s and elicits various responses such as receptor internalization and nuclear import (*3*, *4*). In other cases, HECT-E3 substrates are modified with polyubiquitin (polyUb), a polymer of isopeptide-linked Ub molecules.

Two models have been proposed for the mechanism of formation of polyUb by HECT-E3s (*5*). In the sequential addition model, Ubs are transferred one by one from the active site cysteine on the HECT domain to the growing Ub chain on the substrate. In the indexation model, a polyUb chain builds up on the HECT domain and is transferred in whole to a substrate lysine. Recently published data suggest that the sequential addition model is more general (*6*).

Within the sequential addition model, the number of Ubs that transfer to substrate in a single substrate−E3 binding event will depend on the relative kinetics of E2−E3 binding and unbinding [E2s must disengage from HECT E3s to be recharged by an E1 (*7*)], the E2−E3 transfer step, the E3−substrate transfer step, and the binding lifetime of the E3−substrate complex. If the dissociation rate for E3−substrate binding is slow compared to those of the other processes, it is possible for several Ubs to transfer in a single substrate binding event. In this study, we measure the kinetics and affinities for a key step in this process, the transfer of ubiquitin from E2 UbcH7 to E3 E6AP.

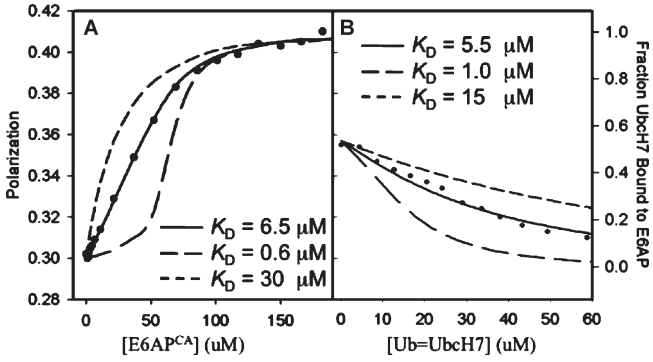

FIGURE 1: Competitive binding titrations show that ubiquitin-charged UbcH7 (UbcH7 = Ub) binds to E6AP with the same affinity as uncharged UbcH7. The fraction of bodipy-UbcH7 bound to E6AP was monitored with fluorescence polarization and measured as a function of E6AP and Ub = UbcH7 concentration. For the left panel, E6AP was titrated into a solution containing 1 μM bodipy-UbcH7 and 80 μM Ub = UbcH7. For the right panel, Ub = UbcH7 was titrated into a solution containing 20 μM E6AP and 20 μM UbcH7 (1 μM labeled with bodipy). In both cases, the data was best fit with dissociation constants for UbcH7 = Ub−E6AP binding (6.5 and 5.5 μM) that closely match the affinity of UbcH7 for E6AP (6.7 μM).

We have previously measured the binding affinity of free E2s for the HECT domain from E6AP (*7*, *8*), but it remains unclear whether the true substrate of E6AP, a Ub∼E2 complex, will bind with greater affinity. Since Ub∼E2 thioester intermediates readily hydrolyze to free Ub and E2, we generated a stable disulfide linkage between the UbcH7 active site cysteine and a Ub protein carrying the G76C mutation (Ub^{C76}) according to the method described by Shaw and co-workers. In the Shaw study, isolated Ub = Ubc1 complexes (= denotes a disulfide bond) were shown to be significantly stabilized over Ub∼Ubc1 complexes while retaining similar interactions at the protein−protein interface (*9*). To generate Ub = UbcH7, we incubated purified Ub^{C76} with a UbcH7 mutant containing only the active site cysteine ($UbcH7^{C86}$) in a buffer promoting disulfide bond formation. The Ub = UbcH7 complex was isolated from unreacted $UbcH7^{C86}$ and Ub^{C76} using size-exclusion chromatography (Figure 1A). When we incubated the Ub = UbcH7 complex with purified E6AP-HECT lacking surface cysteines ($E6AP^{CA}$) at 25 °C for 4 h, we found that the disulfide bond in the Ub = UbcH7 complex remains intact and

*To whom correspondence should be addressed. Phone: (919) 843-0188. Fax: (919) 966-2852. E-mail: bkuhlman@email.unc.edu.

Published on Web 12/29/2009

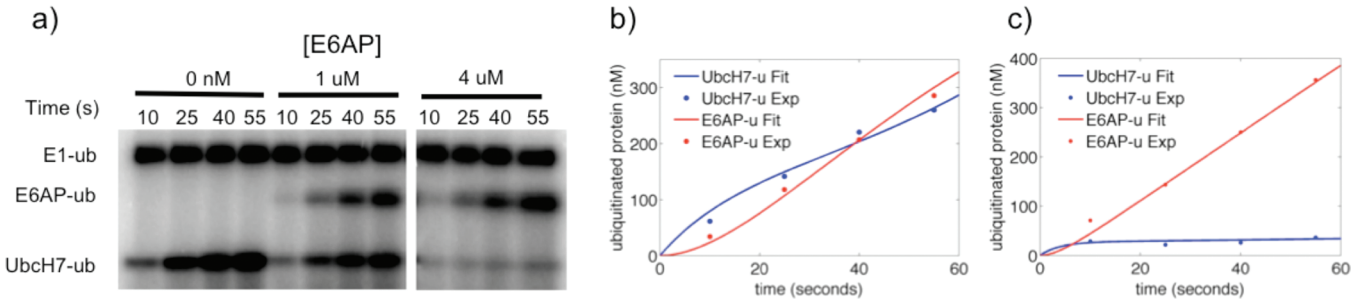

FIGURE 2: Kinetics of UbcH7−E6AP transthiolation at 25 °C. (a) Varying concentrations of E6AP were incubated with ATP, radiolabeled Ub, E1 (500 nM), and UbcH7 (1 μM). (b and c) For each reaction, the buildup of ubiquitin-charged UbcH7 and E6AP was fit using a model with two adjustable parameters: the rate constant for formation of the Ub∼UbcH7 complex from Ub∼E1 and the second-order rate constant (k_{cat}/K_M) for UbcH7−E6AP transthiolation (page 7 of the Supporting Information). In this model, the rate of E6AP ubiquitination at a given time point equals (k_{cat}/K_M)[Ub∼UbcH7][free E6AP]. The fits for 1 μM E6AP (b) and 4 μM E6AP (c) give values of 1.1×10^5 and 1.2×10^5 M^{-1} s^{-1}, respectively, for k_{cat}/K_M.

Ub^{C76} is not transferred to $E6AP^{CA}$ (Figure S2 of the Supporting Information). Subjecting the proteins to β-ME prior to SDS−PAGE shows that the disulfide can be reduced to yield free $UbcH7^{C86}$ and Ub^{C76} proteins.

To measure the binding affinity of Ub = UbcH7 for E6AP, we performed competitive binding experiments with uncharged $UbcH7^{C86}$ labeled with a bodipy dye. Binding of E6AP to bodipy-UbcH7 slows the molecular tumbling rate and increases bodipy fluorescence polarization. First, we measured the affinity of bodipy-$UbcH7^{C86}$ for $E6AP^{CA}$. The measured K_D of 6.7 μM is in good agreement with previous reports of 5 μM for the wild-type interaction (*7*, *8*). Next, we introduced a high concentration of Ub = UbcH7 (80 μM) into the binding titration to act as a competitor for binding of bodipy-$UbcH7^{C86}$ to $E6AP^{CA}$. If the disulfide complex binds with significantly greater affinity, the titrated $E6AP^{CA}$ will preferentially bind to Ub = UbcH7 over bodipy-$UbcH7^{C86}$, resulting in a delayed increase in fluorescence polarization. We did not observe such a lag in our binding experiment, and following analysis with a competitive binding model, we found that the free and Ub-charged UbcH7s bind $E6AP^{CA}$ with indistinguishable affinities (Figure 1 and Table S1). Repeating the experiment with an alternative concentration of Ub = UbcH7 (40 μM) and a variant of E6AP that has only the active site cysteine mutated ($E6AP^{C820A}$) gave similar results (Figure S14). Additionally, we performed the competition experiment by titrating Ub = UbcH7 into a solution containing $E6AP^{C820A}$ and bodipy-$UbcH7^{C86}$ and monitoring the release of bodipy-$UbcH7^{C86}$ (Figure 1). Regression analysis with a competitive binding model again indicated that Ub = UbcH7 does not have enhanced affinity for E6AP.

The rate of transfer of ubiquitin between UbcH7 and HECT-E6AP was probed using multiturnover reactions. E6AP was incubated with ATP, E1, radiolabeled ubiquitin, and UbcH7. At low concentrations of E6AP, the amounts of the Ub∼UbcH7 and Ub∼E6AP complexes grow with time, while at higher E6AP concentrations, the amount of the Ub∼UbcH7 complex rapidly reaches a steady state as the rate of E1−E2 transthiolation equals the rate of UbcH7−E6AP transthiolation (Figure 2). In this scenario, the second-order rate constant for the UbcH7−E6AP transthiolation reaction (k_{cat}/K_M) can be determined by dividing the rate of formation of the Ub∼E6AP complex by the concentration of uncharged E6AP and the steady-state concentration of the Ub∼UbcH7 complex (as determined by phosphoimager analysis of the appropriate bands from the gel). Alternatively, the Ub∼UbcH7 and Ub∼E6AP progress curves can be simultaneously fit by numerical integration with two adjustable parameters: the rate of UbcH7 charging by E1 (k_1[UbcH7], a constant amount of Ub∼E1 complex was observed at all time points) and the second-order rate constant for the UbcH7−E6AP transthiolation reaction (see the Supporting Information for a full description of the fitting process). This approach allows us to fit data in which both Ub∼UbcH7 and Ub∼E6AP levels are changing with time. At E6AP concentrations of > 4 μM, it was not possible to quantify the strength of the Ub∼UbcH7 band, and therefore, K_M could not be measured. In addition to increasing the rate of UbcH7−E6AP transthiolation, a high concentration of E6AP blocks the charging of UbcH7 as the binding of E1 and that of E6AP are mutually exclusive.

Table 1: Dissociation and Kinetic Constants for UbcH7−E6AP Binding and Ubiquitin Transfer

temp (°C)	k_{cat}/K_M (M^{-1} s^{-1})[a]	K_D (μM)[b]
4	$(3.7 \pm 0.1) \times 10^4$	12.5 ± 1.9
25	$(1.2 \pm 0.1) \times 10^5$	6.7 ± 0.7
37	$(2.3 \pm 1.1) \times 10^5$	29 ± 3.3

[a]Errors for k_{cat}/K_m are the standard deviation of multiple experiments. See Table S1 for results from individual experiments. [b]Errors for K_D are errors from the fit.

k_{cat}/K_M and the K_D for binding of UbcH7 to E6AP were measured at 4, 25, and 37 °C (Table 1 and Table S1). At 37 °C, k_{cat}/K_M equals $(2.3 \pm 1.1) \times 10^5$ M^{-1} s^{-1}. The dissociation constant for substrate binding and k_{cat}/K_M place constraints on the minimum value possible for the rate of release of the substrate from E6AP [$k_{off} > K_D(k_{cat}/K_M)$]. At 37 °C, the measured rate constants indicate that k_{off} is greater than 7 s^{-1}.

The rate of transfer of ubiquitin between UbcH7 and E6AP was also probed with pulse−chase single-turnover experiments. The Ub∼E2 complex was generated in a pulse using E1 and ATP, and the reaction was chased with a solution that simultaneously inhibits the E1 and initiates the UbcH7−E6AP transthiolation reaction. In the absence of E6AP, the Ub∼UbcH7 complex remains stable through the course of the reaction (Figure S12). At 25 °C, the reaction was too rapid to detect with manual mixing techniques (first time point at 8 s). At 4 °C, a progressive formation of the Ub∼E6AP complex was observed with a concomitant reduction in the level of the Ub∼UbcH7 complex. Rate profiles at varying concentrations of E6AP (2−40 μM) were globally fit by numerical integration with a model containing three adjustable parameters: the second-order rate constant for

the binding of the Ub∼UbcH7 complex to E6AP (k_{on}), the first-order rate constant for dissociation of the Ub∼UbcH7 complex (k_{off}), and the first-order rate constant for ubiquitin transfer within the bound complex (k_{cat}). The ratio of the on and off rate constants for binding (k_{on} and k_{off}) was held equal to the equilibrium dissociation constant during the fitting process, leaving two floating parameters, k_{on} and k_{cat}. A variety of k_{on} and k_{cat} values, and therefore K_M, fit the data equally well. Reactions at higher concentrations of E6AP that could help to resolve this ambiguity were not informative because the ubqituitin transfer takes place within the dead time of the experiment. All of the low-scoring k_{on} and k_{cat} pairs fit to a common value for k_{cat}/K_M [$k_{cat} \times k_{on}/(k_{on} + k_{off})$]. The value for k_{cat}/K_M was 0.8×10^4 M^{-1} s^{-1}, in modest agreement with the value measured in multiturnover experiments, 3.7×10^4 M^{-1} s^{-1}.

Here we have shown that UbcH7 charged with Ub has an affinity for E6AP similar to that of uncharged UbcH7. Two other studies, both with RING domain E3s, have directly probed the relative affinity of charged and uncharged E2s for E3s. Ub-charged Cdc34 binds Cul1-Rbx1 approximately 2-fold tighter than uncharged E2, and Ub-charged HsUbc2b binds E3α 8-fold tighter (*10*, *11*). In a recently determined crystal structure of the HECT domain of Nedd4 bound to the Ub∼UbcH5b complex, there are direct contacts between the HECT domain and the ubiquitin (*12*). Additionally, mutations to ubiquitin residues that contact the HECT domain slow the rate of UbcH5b−Nedd4 transthiolation with a catalytically crippled UbcH5b. Interestingly, the same mutations to ubiquitin did not have a similar effect on the rate of transthiolation between UbcH5b and E6AP.

For a substrate to be modified by several Ubs in a single E3 binding event, the substrate must remain attached to the E3 longer than it takes the E3 to be recharged with Ub. Intracellular concentrations of charged E2s have been measured in the low micromolar range (*11*). Here, we show that at 37 °C 5 μM Ub∼UbcH7 can charge E6AP at a rate of ∼1 s^{-1}. We also show that the rate of release of UbcH7 from E6AP at 37 °C is > 7 s^{-1}, indicating that the release step should not be the rate-limiting step for multiple transfer events. Therefore, for polyubiquitination to occur via a processive mechanism, the substrate should remain bound to E6AP for more than 1 s. The required lifetime could be even longer, depending on the rate of transfer of ubiquitin between E6AP and substrate. It has been shown that a 16-residue fragment of E6AP binds the substrate-associated protein E6 with a lifetime between 5 and 10 s at 25 °C (*13*). This is consistent with ubiquitination patterns observed in assays with E6AP, E6, and the substrate p53 that are indicative of processive ubiquitination (*6*).

SUPPORTING INFORMATION AVAILABLE

Detailed experimental methods, a summary of kinetic experiments, and fits for all multiturnover and pulse−chase experiments. This material is available free of charge via the Internet at http://pubs.acs.org.

REFERENCES

1. Pickart, C. M., and Eddins, M. J. (2004) Ubiquitin: Structures, functions, mechanisms. *Biochim. Biophys. Acta 1695*, 55–72.
2. Hershko, A., and Ciechanover, A. (1998) The ubiquitin system. *Annu. Rev. Biochem. 67*, 425–479.
3. Bernassola, F., Karin, M., Ciechanover, A., and Melino, G. (2008) The HECT family of E3 ubiquitin ligases: Multiple players in cancer development. *Cancer Cell 14*, 10–21.
4. Rotin, D., and Kumar, S. (2009) Physiological functions of the HECT family of ubiquitin ligases. *Nat. Rev. Mol. Cell Biol. 10*, 398–409.
5. Verdecia, M. A., Joazeiro, C. A., Wells, N. J., Ferrer, J. L., Bowman, M. E., Hunter, T., and Noel, J. P. (2003) Conformational flexibility underlies ubiquitin ligation mediated by the WWP1 HECT domain E3 ligase. *Mol. Cell 11*, 249–259.
6. Kim, H. C., and Huibregtse, J. M. (2009) Polyubiquitination by HECT E3s and the determinants of chain type specificity. *Mol. Cell. Biol. 29*, 3307–3318.
7. Eletr, Z. M., Huang, D. T., Duda, D. M., Schulman, B. A., and Kuhlman, B. (2005) E2 conjugating enzymes must disengage from their E1 enzymes before E3-dependent ubiquitin and ubiquitin-like transfer. *Nat. Struct. Mol. Biol. 12*, 933–934.
8. Eletr, Z. M., and Kuhlman, B. (2007) Sequence determinants of E2-E6AP binding affinity and specificity. *J. Mol. Biol. 369*, 419–428.
9. Merkley, N., Barber, K. R., and Shaw, G. S. (2005) Ubiquitin manipulation by an E2 conjugating enzyme using a novel covalent intermediate. *J. Biol. Chem. 280*, 31732–31738.
10. Saha, A., and Deshaies, R. J. (2008) Multimodal activation of the ubiquitin ligase SCF by Nedd8 conjugation. *Mol. Cell 32*, 21–31.
11. Siepmann, T. J., Bohnsack, R. N., Tokgoz, Z., Baboshina, O. V., and Haas, A. L. (2003) Protein interactions within the N-end rule ubiquitin ligation pathway. *J. Biol. Chem. 278*, 9448–9457.
12. Kamadurai, H., Souphron, J., Scott, D., Duda, D., Miller, D., Stringer, D., Piper, R., and Schulman, B. (2009) Insights into ubiquitin transfer cascades from a structure of a UbcH5B ∼ ubiquitin-$HECT^{NEDD4L}$ complex. *Molecular Cell 36*, 1095–1102.
13. Zanier, K., Charbonnier, S., Baltzinger, M., Nomine, Y., Altschuh, D., and Trave, G. (2005) Kinetic analysis of the interactions of human papillomavirus E6 oncoproteins with the ubiquitin ligase E6AP using surface plasmon resonance. *J. Mol. Biol. 349*, 401–412.